ISBN: 978-3-95450-247-9 ISSN: 2673-5490 doi: 10.18429/JACoW-IPAC2024-TUPS49

ENHANCING PLASMA WAKEFIELD ACCELERATOR ANALYSIS THROUGH MACHINE LEARNING

M. Yadav*, M. H. Oruganti, J. Phillips, B. Naranjo, J. B. Rosenzweig
University of California, Los Angeles, CA, USA

Abstract

An advanced particle-in-cell (PIC) simulation code, QuickPIC, is used to comprehensively analyze beam distributions, particularly those exhibiting perturbations with significant instabilities. To connect simulated beam distributions to physical observables, this study uses cutting-edge neural networks. This research underscores the transformative potential of machine learning (ML) in unraveling plasma wakefield acceleration (PWFA) complexities and enhancing our capabilities in the development of advanced accelerators. Plans for future radiation test using Compton spectrometer are also suggested.

INTRODUCTION

Particle accelerators play a pivotal role in advancing our understanding of fundamental physics. Conventional radio-frequency particle accelerators can only achieve acceleration gradients of approximately 100 MeV/m. To exceed this limit, a range of advanced acceleration techniques have been introduced in various stages of development within the field of accelerator physics. Among these approaches, plasma wakefield acceleration (PWFA) can accelerate particle beams with large gradients TeV/m, efficiency and quality emittance preservation [1–4]. The unique properties of plasma mitigate breakdown issues, utilizing waves excited by an intense drive beam. In turn, these waves are used for the acceleration of a trailing beam. The potential of PWFA applications is now being explored in detail by the global research community, leading to the commissioning of significant facilities dedicated to PWFA research [5–7].

In PWFA, an intense driver beam expels all electrons in the plasma, which are then attracted back on-axis due to the restoring forces of the plasma, resulting in the formation of an electron-free ion column behind the driver bunch known as blowout [8]. This ion column is responsible for the uniform focusing and accelerating fields. Furthermore, it facilitates the diagnosis of beam parameters from the spectral and angular distribution of the betatron radiation, which are essential information regarding the interaction between the beam and plasma [9–12].

In PWFA, where the beam density exceeds the plasma density, the plasma electron response becomes highly nonlinear, resulting in relativistic electron speeds and wave-breaking spike [13–15]. In this paper, one of the focus is on understanding the behavior of perturbed beams within the plasma blowout regime, which is significantly influenced by the properties of the driving particle beam, including its energy, intensity, profile, spot size, and density distribution. Recent publications, such as [10, 16], underscore the community's focus on measurements related to higher intensity beams and emittances during the initial phase of FACET-II research.

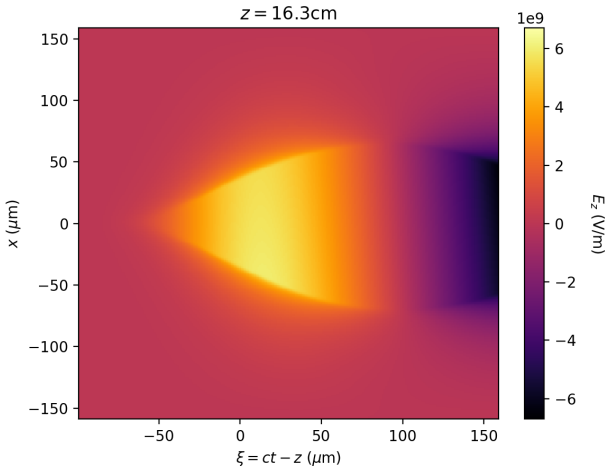

Figure 1: Electric field plot of the beam for semi-Gaussian plasma profile.

In this paper the effects of perturbed beams are presented through the results of PIC simulations. We also discuss how, by running hundreds of parallel simulations, we can train a model that can tell the centroid change of the different banana beams in plasma. We also propose a test experiment at FACET-II to detect radiation in PWFA experiments. Finally, we discuss the implications of our research for experiments at FACET-II and future plasma-based linear colliders are discussed.

PERTURBED BEAMS

The stability of plasma-based accelerators against transverse misalignments and asymmetries of the drive beam is crucial for their applicability. Even small centroid change of the drive beam centroid can couple coherently to the plasma wake grow, and ultimately lead to emittance degradation or beam loss for a trailing witness beam. High-intensity laser pulses or high-density particle bunches to drive a plasma wake. Blowout regime where the driver expels plasma electrons as shown in Fig. 1, leaving an ion cavity with focusing fields. This emphasizes the importance of drive beam stability in plasma accelerators for practical applications.

Figure 2 and Fig. 3 shows the banana beam profiles at 0 cm, 11.9 cm and 14.9 cm in the plasma for two different centroid changes. The plasma profile chosen was a semi-Gaussian ramp with up-ramp 0–10 cm, 10–20 cm uniform

* yadavmonika@physics.ucla.edu

ISBN: 978-3-95450-247-9 ISSN: 2673-5490 doi: 10.18429/JACoW-IPAC2024-TUPS49

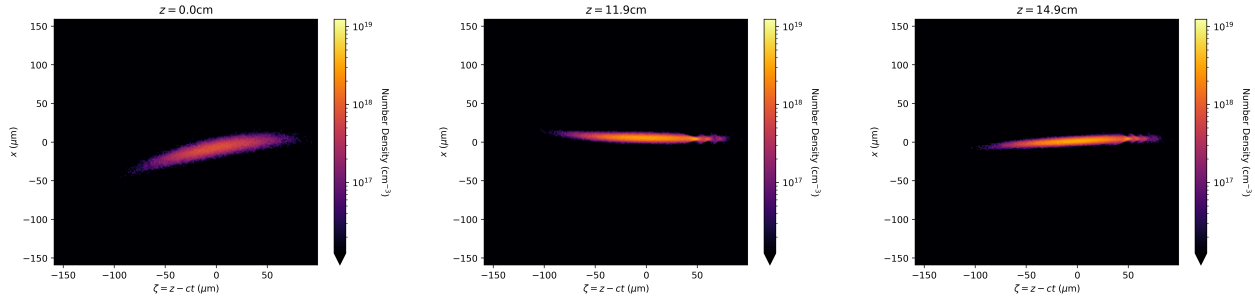

Figure 2: Banana beam profiles at 0 cm , 11.9 cm and 14.9 cm in the plasma. The plasma profile chosen was a semi-Gaussian ramp.

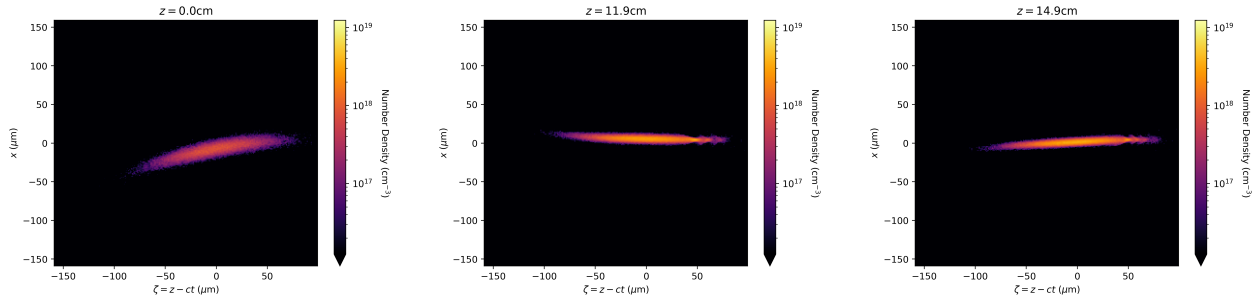

Figure 3: Banana beam offset profiles at 0 cm , 11.9 cm and 14.9 cm in the plasma.

ramp and 20–30 cm downramp. Beam perturbations can often interfere with measurements, reflecting altered distributions in electron beams that add dimensions of increased error to experimental analysis. In plasma lengths exceeding 20 cm, however, there is a self-correcting phenomenon that forces the electron beam to become denser as it passes through the plasma. This allows for beams to be analyzed at a higher quality and with greater certainty, particularly when machine learning can be incorporated into assessing the optimal location of analysis [17, 18].

A promising future direction for this research lies in simulations and large-scale image analysis that leverages the power of convolutional neural networks. By running hundreds of parallel simulations to model how different banana beams will change in plasma, we can train a network to identify the centroid shape of the beam based on a few snapshots in within a certain distance traveled (15–19 cm downstream for example). This can help streamline the analysis of perturbed banana beams and also pave the way for gaining other insights on beam-plasma interactions.

Figure 4 showcases an interesting relationship between a banana beam's centroid parameters and its required stabilization distance. When σ_z is held constant, the distance of stabilization also remains constant despite alterations to parameter "a". Even in the case of significantly changing σ_z and "a", the distance remains the same. Future work can examine with finer resolution exactly how these parameters impact the distance of stabilization or even answer the question of whether they have any impact at all.

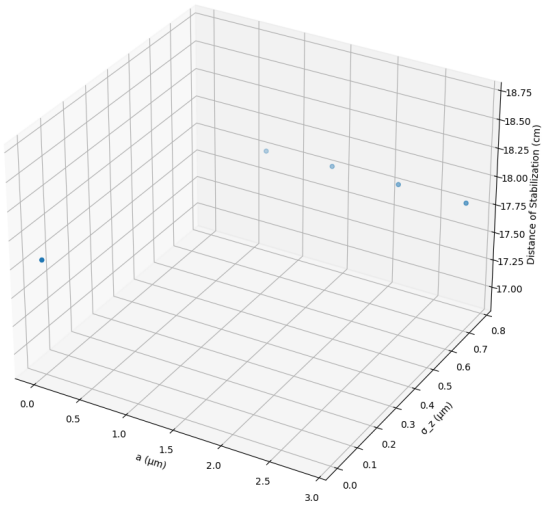

Figure 4: This graph indicates the distance a banana beam must travel through plasma before achieving a stable profile. The independent variables are represented as "a" and σ_z.

DESIGN OF COMPTON SPECTROMETER AT FACET-II

For the initial commissioning of the spectrometer, the region of the IP will be filled with H2 gas with static pressures 5 Torr. At FACET-II, the γ-ray photons are produced at the Interaction Point (IP) where the relativistic electrons interact with matter or with a laser pulse.

As shown in Fig. 5 the design of a Compton spectrometer involves a sextupole for magnetic spectral analysis, covering

ISBN: 978-3-95450-247-9 ISSN: 2673-5490 doi: 10.18429/JACoW-IPAC2024-TUPS49

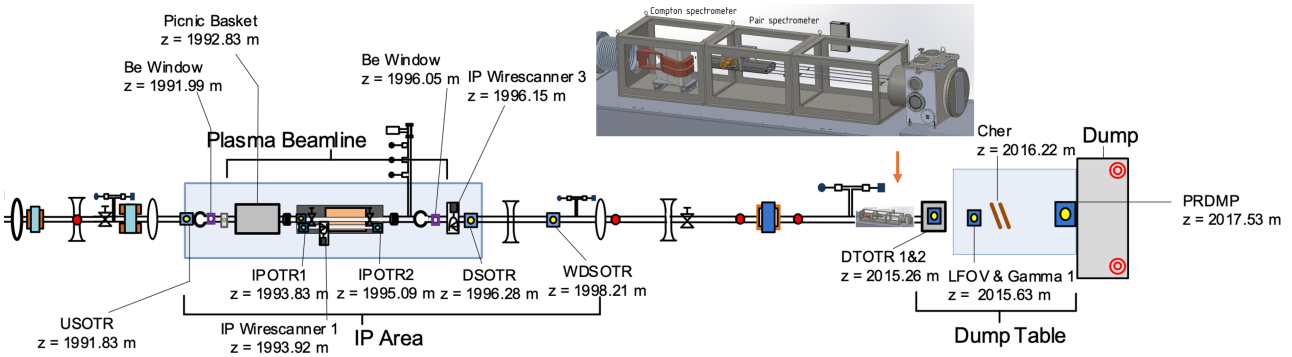

Figure 5: Test experiment at FACET-II will involve detecting radiation using the Compton spectrometer.

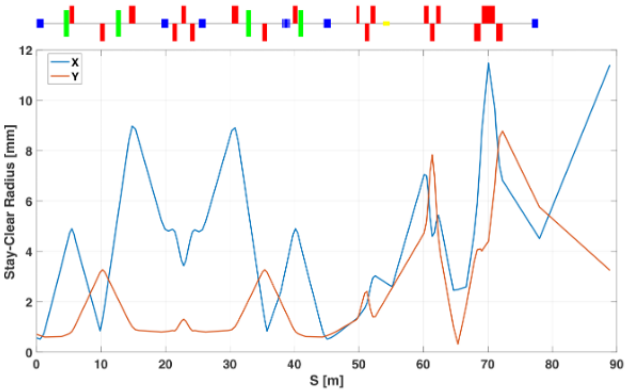

Figure 6: Compton spectrometer stay clear radius using Elegant software.

a dynamic range from few keV to few MeV and capturing energy-angular double-differential electron spectra in a single shot. At electron energies below 1 MeV, where Compton spectroscopy faces challenges due to more isotropic scattering cross-sections, a 3D-printed tungsten collimator is employed at the detector plane to selectively capture forward-scattered electrons. This innovation extends the spectrometer's lower energy limit to approximately 180 keV.

The magnet needs to generate a sextupolar magnetic field to perform momentum analysis on the converted Compton electrons. Interaction of high-energy gamma photons with target materials, gamma photons are converted into high-energy electrons. At this stage, the converted Compton electrons have a wide range of momenta. To perform momentum analysis on these electrons, a sextupolar magnetic field is applied to their path. The sextupolar magnetic field exerts forces on the electrons that vary with their position and momentum. The degree of bending depends on the electron's momentum. Electrons after passing through the sextupolar field, the separated electrons are detected by scintillator screen and cameras. The extent of bending and the position where each electron is detected provides information about its momentum.

The resulting data allows to construct a momentum spectrum, which represents the distribution of electron momenta. At the location of the spectrometer, the photon axis is vertically separated by several millimeters from the dispersed electron axis. The focal plane will be aligned with the scintillator plane and Compton spectrometer stay clear radius is shown in Fig. 6. Spherical silicon nitride bearings of 25 mm diameter will help to roll the CPT spectrometer during translation. All the parts of the spectrometer are assembled and vacuum tests are completed at UCLA. The device will be installed in the summer later this year.

SUMMARY

In conclusion, our study underscores the crucial role of comprehending and controlling perturbations offering valuable insights for applications in advanced technologies. In magnetic Compton spectrometer for SLAC, incident collimated gamma rays strike a converter target, and the resulting scattered Compton electrons are then magnetically analyzed, providing information about the incident gamma beam's spectrum and intensity. Similar spectrometer magnets will be designed for the space plasma experiment at the MITHRA lab. At MITHRA lab, a 30 MeV pulsed electron beam interacts with various targets like plasmas, generating a wide spectrum of electron of 70 MeV. Downstream, the diagnostics beamline captures these electrons, leading to a spot size of just a few millimeters at the spectrometers. Once the beam transport, the plasma source, and the spectrometer are in place, initial measurements will be taken to verify the replication of the Jovian electron spectra.

ACKNOWLEDGEMENT

This work was performed with the support of the US Department of Energy, Division of High Energy Physics, under Contract No. DE-SC0009914, DE-SC0017648, NSF PHY-1549132 Center from Bright Beams, DARPA under Contract N.HR001120C007.

ISBN: 978-3-95450-247-9 ISSN: 2673-5490 doi: 10.18429/JACoW-IPAC2024-TUPS49

REFERENCES

[1] M. Litos *et al.*, "High-efficiency acceleration of an electron beam in a plasma wakefield accelerator," *Nature*, vol. 515, pp. 1476–4687, 2014. doi:10.1038/nature13882

[2] I. Blumenfeld *et al.*, "Energy doubling of 42 GeV electrons in a metre-scale plasma wakefield accelerator," *Nature*, vol. 445, no. 7129, pp. 741–744, 2007. doi:10.1038/nature05538

[3] C. Lindstrøm and M. Thévenet, "Emittance preservation in advanced accelerators," *Journal of Instrumentation*, vol. 17, no. 05, P05016, 2022. doi:10.1088/1748-0221/17/05/P05016

[4] C. A. Lindstrøm *et al.*, "Energy-spread preservation and high efficiency in a plasma-wakefield accelerator," *Phys. Rev. Lett.*, vol. 126, p. 014 801, 1 2021. doi:10.1103/PhysRevLett.126.014801

[5] H. Wiedemann, *Particle Accelerator Physics*. Springer, Cham, 2015. doi:https://doi.org/10.1007/978-3-319-18317-6

[6] J. D. Jackson, *Classical electrodynamics*, und, 12. print. Wiley, 1962.

[7] K.-J. Kim, Z. Huang, and R. Lindberg, "Synchrotron radiation," in *Synchrotron Radiation and Free-Electron Lasers: Principles of Coherent X-Ray Generation*. 2017, pp. 33–73. doi:10.1017/9781316677377.003

[8] J. B. Rosenzweig *et al.*, ""acceleration and focusing of electrons in two-dimensional nonlinear plasma wake fields"," *Phys. Rev. A*, vol. 44, R6189–R6192, 10 1991. doi:10.1103/PhysRevA.44.R6189

[9] H. Suk *et al.*, "Plasma electron trapping and acceleration in a plasma wake field using a density transition," *Phys. Rev. Lett.*, vol. 86, pp. 1011–1014, 6 2001. doi:10.1103/PhysRevLett.86.1011

[10] V. Yakimenko *et al.*, "FACET-II facility for advanced accelerator experimental tests," *Phys. Rev. Accel. Beams*, vol. 22, p. 101 301, 10 2019. doi:10.1103/PhysRevAccelBeams.22.101301

[11] S. Corde *et al.*, ""femtosecond x rays from laser-plasma accelerators"," *Rev. Mod. Phys.*, vol. 85, pp. 1–48, 1 2013. doi:10.1103/RevModPhys.85.1

[12] T. Tajima and J. M. Dawson, "Laser electron accelerator," *Phys. Rev. Lett.*, vol. 43, pp. 267–270, 4 1979. doi:10.1103/PhysRevLett.43.267

[13] W. Lu *et al.*, "Nonlinear theory for relativistic plasma wakefields in the blowout regime," *Phys. Rev. Lett.*, vol. 96, p. 165 002, 16 2006. doi:10.1103/PhysRevLett.96.165002

[14] W. Lu *et al.*, "A nonlinear theory for multidimensional relativistic plasma wave wakefieldsa)," *Physics of Plasmas*, vol. 13, no. 5, p. 056 709, 2006. doi:10.1063/1.2203364

[15] K. V. Lotov, "Blowout regimes of plasma wakefield acceleration," *Phys. Rev. E*, vol. 69, p. 046 405, 4 2004. doi:10.1103/PhysRevE.69.046405

[16] C. Joshi *et al.*, "Plasma wakefield acceleration experiments at FACET II," *Plasma Physics and Controlled Fusion*, vol. 60, no. 3, p. 034 001, 2018. doi:10.1088/1361-6587/aaa2e3

[17] M. Yadav *et al.*, *Machine learning-based analysis of experimental electron beams and gamma energy distributions*, 2023.

[18] M. Yadav *et al.*, "Machine learning-based spectrum reconstruction and modeling beam perturbation effects on betatron radiation," *Preprints*, 2023. doi:10.20944/preprints202310.1129.v1